Coexistence Curve of the Ionic Binary Mixture Ethylammonium Nitrate−*n*-Octanol: Critical Properties

M. Bonetti* and A. Oleinikova†

Service de Physique de l'Etat Condensé, Commissariat à l'Energie Atomique, Orme des Merisiers, 91191 Gif sur Yvette, France

C. Bervillier

Service de Physique Théorique, Commissariat à l'Energie Atomique, Orme des Merisiers, 91191 Gif sur Yvette, France

Received: July 31, 1996[⊗]

We present measurements of the coexistence curve of the ionic mixture ethylammonium nitrate - *n*-octanol within the reduced temperature range $2.6 \times 10^{-5} < t < 4.2 \times 10^{-2}$. The salt volume fraction is chosen as the order parameter as this gives the most symmetric phase diagram. The determination of the asymptotic critical exponent β gives a value close to the 3-D Ising value although correction-to-scaling terms are necessary to fit the data. The effective exponent β_{eff} as a function of the reduced temperature does not show any crossover from the classical to the Ising value and suggests rather an approach, *from below*, to the asymptotic 3-D Ising value. The $(1 - \alpha)$ anomaly of the mean diameter could not be precisely determined although a deviation near T_c from the rectilinear law could be noticed.

I. Introduction

Knowledge of the thermodynamic properties of ionic fluids near the critical point is an active area of research.[1−4] One of the main goals is to determine whether ionic systems belong to the same universality class as pure fluids and nonionic binary mixtures which are usually thought to have an Ising-type asymptotic behavior.

Ionic binary systems composed of a completely dissociated salt within a solvent are true electrolytes and are classified as *ionophores* (intrinsic electrolytes), in contrast to *ionogens* (potential electrolytes) for which one component dissociates partially into ions in the presence of the solvent.[5]

The range of intermolecular forces in ionic binary systems seems to be one of the main factors which may modify the nature of the critical behavior. Long range electrostatic forces (Coulombic forces) are large particularly in systems with a low value of the dielectric constant ($\epsilon \leq 10$) of the solvent.[2,3] These systems (coined Coulombic systems) seem to be better described by mean-field critical exponents although a crossover to an Ising-type behavior might be localized in a nonaccessible experimental temperature region very close to the critical point. When the value of the dielectric constant of the solvent is increased, the temperature range within which an Ising-type behavior is observed increases as indicated by recent measurements of Narayanan *et al.*[6]

Phase separation in ionic systems may be classified[7,8] as *Coulombic unmixing*, for which a strong peak in the pair-correlation function between ions with opposite signs is observed as shown by recent small angle neutron scattering,[9,10] or *solvophobic unmixing* where, at the contrary, the pair-correlation function between ions with the same sign has the largest value.[11] Solvophobic systems have been shown to belong to the Ising-type universality class.[3,12] Short range interactions such as hydrogen bonding as well as asymmetry of the ions may drive ionic binary mixtures, which would be expected to be mean-field, into the Ising-type universality class.[3] Among these latter systems, the binary ionic mixture, ethylammonium nitrate (EAN)[13,14] in a low dielectric solvent ($\epsilon \simeq 8$), *n*-octanol, appears to show an Ising-type criticality.[15,16]

The coexistence curve has been studied for different binary ionic systems. We recall here the main results concerning the value of the critical exponent β which describes the shape of the coexistence curve near the critical point. Water solutions of tetra-*n*-pentylammonium bromide[12] (Pe_4NBr) and propyl-tributylammonium iodide[17] give a value close to the 3-D Ising value, $\beta = 0.325$. The shape of the coexistence curve of electrolytes in solvents with a low value of the dielectric constant was investigated by Pitzer *et al.*[18] with a mixture of tetra-*n*-butylammonium picrate and 1-chloroheptane and by Singh *et al.*[19,20] with a mixture of triethyl-*n*-hexylammonium triethyl-*n*-hexylboride ($HexEt_3N$ $HexEt_3B$) and diphenyl ether. These systems can be described in terms of the classical value $\beta = 0.5$ although the work of Singh *et al.*[20] shows a possible crossover of the effective exponent β_{eff} from the classical to the asymptotic 3-D Ising value when the Ising β value is imposed in the fitting procedure.

In this paper we present measurements of the coexistence curve of the binary mixture EAN−*n*-octanol. This ionic mixture has an upper critical consolute point in the salt-rich domain. This may be attributed in part to clustering between ions through hydrogen bonds.[3,17] In spite of a low value of the dielectric constant, the system shows an Ising-type critical behavior.[15,16] Viscosity measurements performed on this system (see ref 21 and references therein) follow the predictions of the dynamic renormalization group and the mode-coupling theories developed for nonionic fluids, and, in order to correctly describe the critical anomaly of the shear viscosity, it appears that corrections to scaling are necessary. The present paper focuses on careful fits of the coexistence curve in order to determine the effective exponent β_{eff} as a function of the temperature. Comparison is

* Address correspondence to this author.
† Permanent address: Physics Department, T. Shevchenko University, 6, Glushkov pr., Kiev, 252127 Ukraine.
⊗ Abstract published in *Advance ACS Abstracts,* February 15, 1997.

S1089-5647(96)02316-4 CCC: $14.00

then made with available coexistence curve data of electrolytic systems belonging either to the Coulombic or to the solvophobic classes.

II. Experimental Section

Sample Preparation. The salt ethylammonium nitrate (EAN) was prepared by neutralizing ethylamine (Aldrich) with nitric acid (Aldrich).[13,22] The salt was dried in a vacuum desiccator with P_2O_5 at ambient temperature for 10 days, filtered through a Millipore filter, and kept frozen at 6 °C. EAN is a fused salt at ambient temperature with a melting temperature at ≃14 °C. The solvent *n*-octanol (Aldrich, water content <0.01%, glass distilled) was used without further purification. A high-precision square cell ($\theta = 90° \pm 2'$) (Hellma GmbH & Co., Germany) with quartz walls was repeatedly washed with Milli-Q water and dried under vacuum at 80 °C. The cell was filled at the critical salt mole fraction $x_{s,c} = 0.766 \pm 0.002$[16,21] under a dry argon atmosphere in a glovebox and sealed with a Teflon screw tap.

Coexistence Curve Measurements. The coexistence curve was obtained by measuring the refractive index of each phase within the two-phase region. The principle of the minimum deviation of a laser beam was used.[23,24] The cell was immersed in a water bath with a temperature stability better than 0.5 mK. In order to determine the minimum deviation angle α of the laser beam as it is transmitted through the upper and lower phases, the cell is vertically supported by a goniometer. From the value of the angle α, the refractive index *n* of each phase (at the wavelength $\lambda = 632.8$ nm) is determined from the following:

$$n = n_w \frac{\sin\left(\frac{1}{2}(\theta + \alpha)\right)}{\sin\left(\frac{1}{2}\theta\right)} \quad (1)$$

where $\theta = 90°$ is the angle between the windows of the cell and n_w is the refractive index of water at $\lambda = 632.8$ nm, whose temperature dependence is given by the following:[24]

$$n_w = 1.331904 - 9.083295 \times 10^{-5}(T - T_0)[1 + 1.49864 \times 10^{-2}(T - T_0) - 2.479132 \times 10^{-5}(T - T_0)^2] \quad (2)$$

with an accuracy $\delta n_w \simeq 10^{-5}$ and with T, the water temperature (in °C) and $T_0 = 18.0859$ °C. In the present measurements, the relative accuracy of the refractive index is $\delta n_r \simeq 2 \times 10^{-5}$ and the absolute accuracy is $\delta n \simeq 2 \times 10^{-4}$.[24] The refractive index of each phase could be measured by vertically displacing the cell. In order to reduce the equilibration time due to the high viscosity of the fluid sample[21] and to avoid concentration gradients within the fluid, we used a sample height of ≈1 cm. The refractive index for each temperature was measured as follows. The fluid was vigorously shaken only when the temperature equilibration of the sample was reached. Due to the large density difference between EAN and *n*-octanol ($\Delta\rho \simeq 0.38$ g/cm^3), phase separation was completed within 24 h. Each phase appears then transparent with no inhomogeneity. However, very near T_c, longer equilibration times were needed for a complete phase separation (up to 2 days). The temperature dependence of the refractive index of each phase was measured by increasing the temperature from the ambient temperature to the critical temperature T_c. The critical temperature T_c was obtained by observing the appearance of a *spinodal decomposition* ring in the forward scattered light after a 3 mK temperature quench (from $T = 41.790$ °C to 41.787 °C) across the coexistence curve. Criticality of the fluid sample was checked by the formation of the meniscus in the middle of the fluid sample height. The estimated critical temperature is $T_c = 41.788_5$ °C ± 1.5 mK. The measured refractive indices of the upper "octanol-rich" and lower "salt-rich" phases as a function of the temperature are reported in Table 1. We also report the refractive index in the one-phase region above T_c at the critical concentration. These high-temperature points (up to $T = 48.586$ °C) were obtained after the two-phase measurements were completed in such a way as to preserve the sample from any possible salt decomposition.

Sample Homogeneity. In our experience an equilibration time of 24 h (up to 48 h near T_c) was sufficient to obtain a complete phase separation. In the following we give an estimation of some characteristic times which govern the dynamics of demixing and sedimentation of the binary mixture in the two-phase state.

Shaking the fluid cell vertically induces a strong shear which is estimated to be $\gamma \approx 30$ s^{-1}. Droplets with different salt concentrations are formed within the fluid with a characteristic length $l_s = (\nu/\gamma)^{1/2}$, where ν is the kinematic viscosity. Typically, the smallest size achieved is $l_s \approx 0.5-1$ mm. Gravity-induced sedimentation is initiated when the size R of the droplets is of the order of the capillary length $l_c = (\sigma/(g\Delta\rho))^{1/2}$, where σ is the interfacial tension and $\Delta\rho$ is the density difference between the coexisting phases.[25,26] Near T_c the capillary length goes to zero as $t^{\nu-(\beta/2)}$ with $t = (T_c - T)/T_c$, $\nu = 0.64$ and $\beta = 0.325$ the critical exponents of the correlation length and of the coexistence curve, respectively. Estimation of the capillary length for the EAN−*n*-octanol mixture gives $l_c \approx 0.5$ mm at $t = 10^{-5}$. Actually, shaking the sample cell induces the formation of droplets of size l_s which start immediately to settle under gravity. Droplets are rapidly convected through the fluid sample: domains of denser (lighter) fluid go to the bottom (top) of the fluid cell. A gravity-induced sedimentation velocity can be estimated from Stokes law, $V_s = 2g\Delta\rho R^2/9\eta$, where η is the viscosity. With $R = l_s$, $V_s \approx 1$ cm/s. This droplet sedimentation induces a hydrodynamic flow favoring the coalescence of droplets at the meniscus. The time of coalescence is difficult to quantify. Recent experiments in a near critical mixture of isobutyric acid and water have shown that the final equilibrium between the phases is achieved for $t \geq 500$ s.[27] It appears therefore that the demixing dynamics is a rapid process. Thus, points near T_c have been measured in an equilibrium state.

In order to check the homogeneity of the sample, refractive index measurements for a reduced temperature down to $t = 2.6 \times 10^{-5}$ have been made at two points in each phase, respectively, at 0.5 and 2.5 mm from the position of the meniscus. Within our experimental uncertainty, gravity-induced concentration gradients[28,29] in our binary mixtures could not be detected.

Accuracy of the Refractive Index Measurement. Wiggles on the coexistence curve may be observed (see Figure 1). This might come from the fact that, in order to strongly mix the fluid, the cell is dismounted from the support, shaken vertically, and actually repositioned on its support. This is repeated at each temperature. When it is repositioned, the cell may not be exactly at the same initial position. This might give a slight shift of the laser beam which induces an absolute error of the refractive index $\delta n \simeq 2 \times 10^{-4}$ ($\delta\phi \approx 0.5-1\%$, ϕ being the salt volume fraction).

Order Parameter. In Figure 1, we show the variation of the refractive index of each phase as a function of temperature. With the refractive index as the order parameter, the coexistencecurve appears rather asymmetric. Coexistence curves obtained by using the salt composition expressed in volume

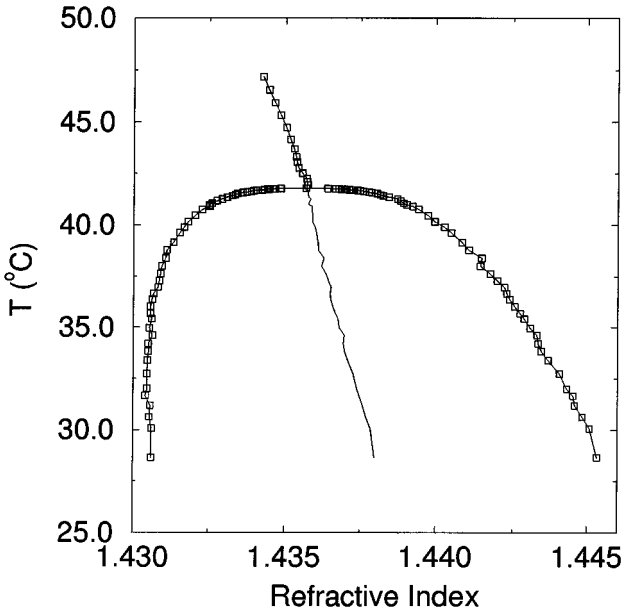

Figure 1. Refractive indices of the two phases of the mixture ethylammonium nitrate−*n*-octanol as a function of temperature. The solid line represents the mean diameter.

fraction, mass fraction, and mole fraction are presented in Figure 2. Conversion of the refractive index to the salt composition in each phase was obtained from the Lorentz−Lorenz (L−L) relation applied to each phase and assuming no excess volume effect.[23,24,30] Indeed, Oleinikova *et al.*[21] have shown that no critical $(1 - \alpha)$ volume anomaly (with $\alpha = 0.11$, the critical exponent of the specific heat c_p) could be detected for $10^{-4} \leq t$. As will be shown in the analysis of the rectilinear mean diameter (Section III.C), the assumption of the volume additivity is verified, within 0.4% (comparable to the $\delta\phi$ error ~1%), for the temperature range $9 \times 10^{-3} < t < 4.2 \times 10^{-2}$.

The temperature dependence of the refractive index of each pure component was measured separately in the same square cell (at $\lambda = 632.8$ nm) within the temperature range 30−48 °C and reads

$$n_{oct} = 1.29727 + (37.88916/T), \qquad n\text{-octanol}$$

$$n_{EAN} = 1.37596 + (21.72773/T), \qquad \text{ethylammonium nitrate}$$

where T is the sample temperature in K. From Figure 2, part a, we see that the salt volume fraction, taken as the order parameter, gives the more symmetrical coexistence curve. Hence, it is the most appropriate order parameter for the subsequent analysis.[29] The salt volume fraction computed for both phases as a function of temperature is reported in Table 1.

III. Data Analysis

The critical exponent β defines the asymptotic shape of the coexistence curve $\Delta\Phi = (\phi_{s,l} - \phi_{s,u})/2\phi_c = B_0 t^\beta$, where $\phi_{s,l}$ and $\phi_{s,u}$ are respectively the salt volume fraction in the lower salt-rich and upper octanol-rich phases, ϕ_c is the critical salt volume fraction, and $t = (T_c - T)/T_c$ is the reduced temperature. Within a large temperature domain, correction-to-scaling terms[31] may be added and are usually introduced as follows:[31,32]

$$\Delta\Phi = B_0 t^\beta (1 + B_1 t^\Delta + B_2 t^{2\Delta} + ...) \qquad (3)$$

where $\Delta = 0.5$ is supposed to be a universal exponent and the B_i's are system dependent correction-to-scaling amplitudes to be determined by a fitting procedure. The χ^2 goodness-of-fit

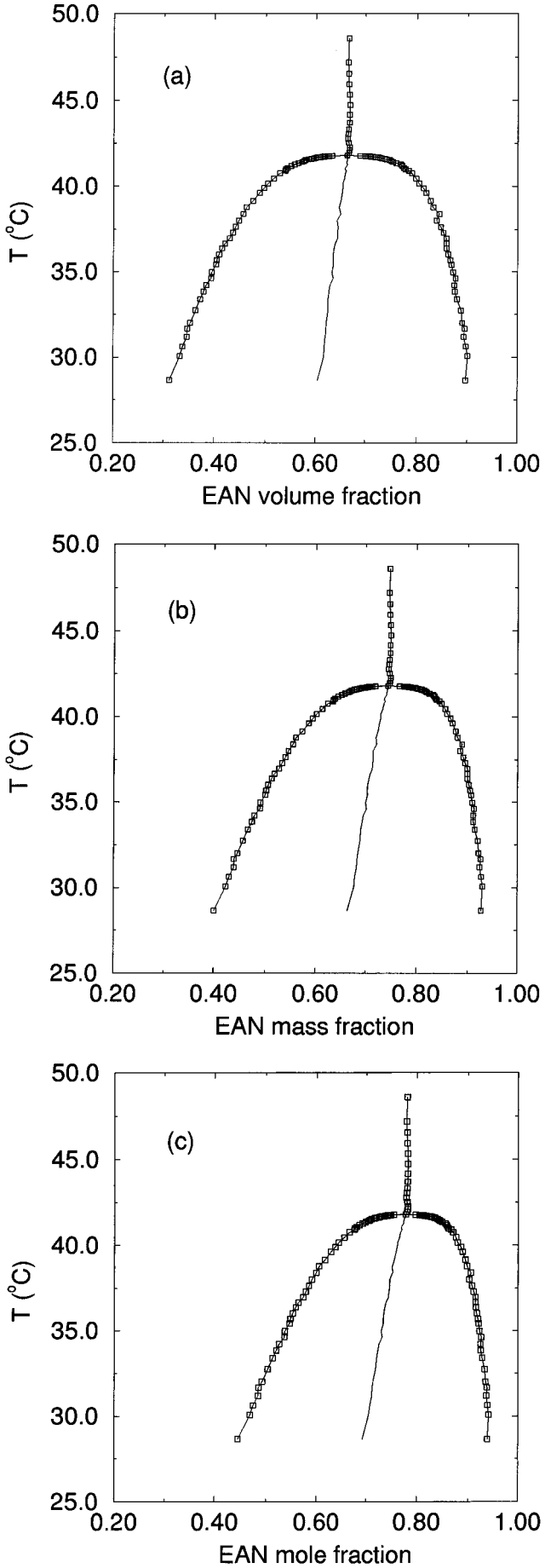

Figure 2. Coexistence curves of the mixture ethylammonium nitrate−*n*-octanol as a function of temperature. Salt composition: (a) salt volume fraction, (b) salt mass fraction, and (c) salt mole fraction. The solid line represents the mean diameter.

TABLE 1: Refractive Indices n_u and n_l, Salt Volume Fractions $\phi_{s,u}$ and $\phi_{s,l}$ in the Upper (*n*-Octanol-Rich Phase) and Lower (EAN-Rich Phase) Phases, and Mean Diameters $\langle x_s \rangle$ Computed from the Salt Mole Fraction as a Function of Temperature[a]

T (°C)	n_u	n_l	$\Phi_{s,u}$	$\Phi_{s,l}$	$\langle x_s \rangle$
28.6578	1.43060	1.44533	0.31172*	0.89655*	0.69240
30.0767	1.43061	1.44507	0.33228*	0.90059*	0.70542
30.6302	1.43055	1.44483	0.33762	0.89670	0.70724
31.1931	1.43057	1.44458	0.34616*	0.89254*	0.71073
31.6770	1.43041	1.44452	0.34651	0.89495	0.71170
32.0160	1.43046	1.44430	0.35305	0.88977	0.71370
32.7334	1.43046	1.44406	0.36266*	0.88749*	0.71827
33.3855	1.43047	1.44367	0.37167*	0.87885*	0.72046
33.8440	1.43050	1.44344	0.37882*	0.87449*	0.72292
34.2081	1.43050	1.44334	0.38354	0.87418	0.72534
34.6217	1.43063	1.44329	0.39382*	0.87623*	0.73140
34.9755	1.43053	1.44306	0.39450*	0.87088*	0.73010
35.4270	1.43061	1.44287	0.40326*	0.86798*	0.73374
35.6800	1.43057	1.44274	0.40492	0.86547	0.73382
36.0246	1.43057	1.44255	0.40921*	0.86157*	0.73480
36.3705	1.43062	1.44238	0.41539*	0.85845*	0.73698
36.6496	1.43067	1.44229	0.42072*	0.85771*	0.73945
36.9605	1.43081	1.44221	0.42979*	0.85763*	0.74400
37.2881	1.43085	1.44198	0.43527*	0.85210*	0.74498
37.6390	1.43090	1.44175	0.44136*	0.84682*	0.74631
38.0090	1.43094	1.44143	0.44727*	0.83837*	0.74650
38.3892	1.43106	1.44147	0.45625*	0.84340*	0.75252
38.7748	1.43110	1.44105	0.46227*	0.83144*	0.75156
39.1580	1.43132	1.44082	0.47489*	0.82651*	0.75599
39.6148	1.43153	1.44048	0.48791*	0.81823*	0.75941
39.9000	1.43167	1.44026	0.49632*	0.81279*	0.76153
40.1651	1.43181	1.43995	0.50448*	0.80388*	0.76232
40.4580	1.43204	1.43973	0.51622*	0.79855*	0.76589
40.7468	1.43227	1.43942	0.52787*	0.78990*	0.76821
40.9081	1.43252	1.43922	0.53881*	0.78410*	0.77109
40.9925	1.43251	1.43902	0.53936*	0.77759*	0.76910
41.0713	1.43259	1.43892	0.54315*	0.77468*	0.76977
41.1690	1.43275	1.43882	0.55007*	0.77196*	0.77186
41.2725	1.43292	1.43871	0.55740*	0.76892*	0.77400
41.3664	1.43309	1.43843	0.56463*	0.75959*	0.77386
41.4254	1.43326	1.43824	0.57147*	0.75323*	0.77455
41.4717	1.43335	1.43814	0.57526*	0.75003*	0.77503
41.5229	1.43343	1.43804	0.57872*	0.74687*	0.77538
41.5714	1.43360	1.43786	0.58544*	0.74078*	0.77604
41.6106	1.43373	1.43776	0.59060*	0.73751*	0.77703
41.6440	1.43387	1.43758	0.59606*	0.73128*	0.77706
41.6640	1.43395	1.43748	0.59918*	0.72783*	0.77711
41.6860	1.43404	1.43739	0.60270*	0.72477*	0.77745
41.7068	1.43422	1.43721	0.60948*	0.71842*	0.77792
41.7195	1.43431	1.43711	0.61289*	0.71490*	0.77803
41.7295	1.43431	1.43702	0.61299*	0.71172*	0.77690
41.7360	1.43440	1.43697	0.61634*	0.70997*	0.77762
41.7421	1.43440	1.43693	0.61641*	0.70857*	0.77713
41.7462	1.43440	1.43684	0.61645*	0.70534*	0.77595
41.7541	1.43448	1.43684	0.61945*	0.70541*	0.77720
41.7612	1.43457	1.43675	0.62280*	0.70221*	0.77736
41.7691	1.43466	1.43665	0.62616*	0.69865*	0.77739
41.7802	1.43484	1.43638	0.63283*	0.68893*	0.77642
T (°C)		n	Φ_s		x_s
41.7920		1.43566	0.66283		0.77824
41.7942		1.43566	0.66285		0.77826
41.7954		1.43566	0.66279		0.77822
41.7977		1.43566	0.66289		0.77829
41.9466		1.43572	0.66656		0.78113
42.1000		1.43570	0.66736		0.78176
42.2590		1.43568	0.66821		0.78242
42.5170		1.43555	0.66604		0.78077
42.7790		1.43542	0.66393		0.77916
43.0460		1.43537	0.66475		0.77980
43.3170		1.43533	0.66597		0.78076
43.7030		1.43527	0.66757		0.78202
44.1500		1.43515	0.66761		0.78208
44.7220		1.43502	0.66846		0.78277
45.3120		1.43484	0.66769		0.78221
45.9220		1.43465	0.66673		0.78151
46.5380		1.43446	0.66582		0.78085
47.1740		1.43426	0.66472		0.78005
48.5860		1.43394	0.66658		0.78156

[a] Critical temperature: $T_c = 41.788_5$ °C. Data points labeled by an asterisk are used when fitting the coexistence curve. In the one-phase region, for T > T_c, the refractive index n is measured at the location where the meniscus should form. ϕ_s = salt volume fraction and x_s = salt mole fraction in the one-phase region.

test was used to optimize the fit and is defined as the following:

$$\chi^2 = \frac{1}{N-M}\sum_{i=1}^{N}\left(\frac{y_i - y(a_1, ..., a_M)}{\sigma_i}\right)^2 \qquad (4)$$

where $(N - M)$ is the number of degrees of freedom with N being the number of data points $y_i = \Delta\Phi(T_i)$, M being the number of fitted parameters a_i in the function $y(a_1, ..., a_M)$, and σ_i being the variance of y_i. The error $\delta\phi = (\partial\Delta\Phi/\partial t)\delta t$ due to the temperature uncertainty ($\delta T \simeq 0.5$ mK) is smaller by 1 order of magnitude, at $t \approx 10^{-4}$, compared to the estimated error $\delta\phi \simeq 1\%$. Hence, the propagation of the temperature uncertainty is not important in our data, and the variance is estimated as $\sigma_i \simeq 1\% \times \Delta\Phi(T_i)$.

The residuals (%) are defined as $(y_i - y(a_1, ..., a_M))/y_i$. Points (labeled by an asterisk in Table 1) with a logarithmic temperature step $\log(\Delta t) = 0.05$ have been chosen for the fit with eq 3.

We present in the following an analysis performed over two data sets: a *full* data set contains 48 points within a temperature interval of $2.6 \times 10^{-5} < t < 4.2 \times 10^{-2}$ and a *reduced* data set with 44 points which spans the temperature interval $1 \times 10^{-4} < t < 4.2 \times 10^{-2}$ (4 data points are skipped very near T_c). The choice of a reduced data set will be made clearer when looking at Figure 7 which shows some systematic deviation of the residuals very near T_c, not compatible with the general trend. With both data sets, the fits give similar values of the B_i amplitudes. Moreover, the trend of the effective exponent β_{eff} (see section III.B) as a function of the reduced temperature t are not dependent on the chosen data set.

Near T_c, the largest absolute error of $\Delta\Phi$ is estimated to be ~1% (see also the analysis of the mean diameter of the coexistence curve, section III.C). In our fitting analysis, the dispersion of the residuals is generally found between ±2% for good fits and ±4% otherwise.

III.A. Critical Exponent β and Correction to Scaling. Two kinds of fits[33] have been performed: on one hand, the critical temperature T_c and the critical exponent β are allowed to vary; on the other hand, they are set fixed, at $T_c = 41.788_5$ °C and to the 3-D Ising value $\beta = 0.325$ (see for example Zinn-Justin[34] and references therein). In both cases, up to two correction-to-scaling terms were used.

Full Data Set (48 Data Points). In Table 2, fits 1-a, 2-a, and 3-a are obtained using a pure power law and a power law with one correction- and two correction-to-scaling terms, respectively. The temperature is set to the experimental $T_c = 41.788_5$ °C and $\beta = 0.325$. The χ^2 error decreases as the number of correction-to-scaling terms increases. Figure 3 shows the residuals from the fit with two correction-to-scaling terms. One notices that the residuals for the four points near T_c are not compatible with the trend of the other points (for $t > 10^{-4}$) which shows some kind of curvature.

In order to diminish the scatter in the residuals, we let free the critical temperature and the β exponent (fits 1-a to 3-a in Table 3). The residuals from the fits with a pure power law and a power with two correction-to-scaling terms are shown in Figure 4, parts a and b, respectively. Although the pure power law gives acceptable values for T_c and β, the residuals are not homogeneously distributed. With two correction-to-scaling terms, the dispersion becomes more uniformly distributed but both the T_c and β values given by the fit are large compared to the experimental T_c and the 3-D β-Ising values.

This fact led us to reduce the temperature interval in order to study the dependence of the fitting parameters on the temperature range.

TABLE 2: Values of the Parameters Obtained by Fitting the Coexistence Curve with $\Delta\Phi = (B_0\, t^{\beta}(1 + B_1\, t^{\Delta} + B_2\, t^{2\Delta})$, See Text[a]

fit	no. of points	T_c (°C)	β	B_0	B_1	B_2	Δ	χ^2
1-a	48	(41.788_5)	(0.325)	1.248 ± 0.012				1.10
2-a	48	(41.788_5)	(0.325)	1.245 ± 0.012	0.031 ± 0.10		(0.5)	1.11
3-a	48	(41.788_5)	(0.325)	1.235 ± 0.012	0.361 ± 0.11	-1.80 ± 0.7	(0.5)	1.03
1-b	44	(41.788_5)	(0.325)	1.246 ± 0.019				1.05
2-b	44	(41.788_5)	(0.325)	1.239 ± 0.019	0.072 ± 0.16		(0.5)	1.00
3-b	44	(41.788_5)	(0.325)	1.219 ± 0.019	0.645 ± 0.16	-3.04 ± 1.0	(0.5)	0.71

[a] T_c, β, and Δ (in parentheses) are held fixed in the fitting. Parameter uncertainties are for one standard-deviation.

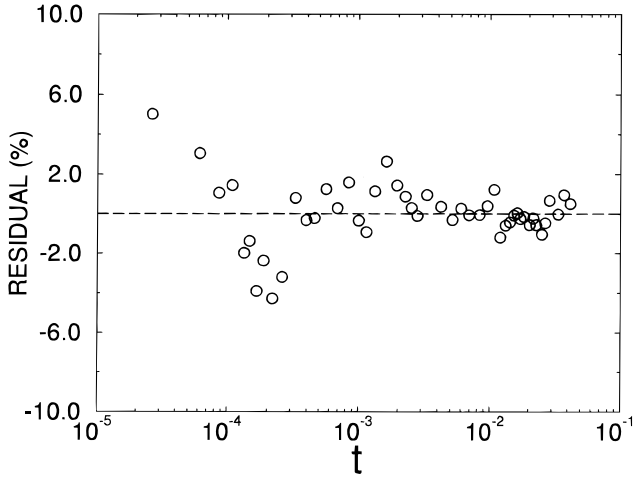

Figure 3. Residuals plot from the fit of the salt volume fraction $\Delta\Phi$ as a function of the reduced temperature t (*full data set*). Fitting with a power law and two correction-to-scaling terms, eq 3 (fit 3-a, Table 2). $T_c = 41.788_5$ °C and $\beta = 0.325$ are fixed parameters in the fit.

Reduced Data Set (44 Data Points). Fitting with a pure power law (without correction-to-scaling terms) with T_c to the experimental value 41.788_5 °C gives a critical exponent $\beta = 0.329 \pm 0.002$, close to the 3-D Ising value, with an amplitude $B_0 = 1.276 \pm 0.02$. One notices some curvature in the residuals plot (Figure 5, part a) which suggests the need for corrections to scaling.

Table 2 (fits 1-b, 2-b, and 3-b) shows the result of the fit with T_c fixed at the experimental value 41.788_5 °C and with $\beta = 0.325$ for a pure power law and for a power law with one and two correction-to-scaling terms. From Table 2, the χ^2 decreases as more terms of correction to scaling are added. Figure 5, part b, shows the residuals as a function of the reduced temperature t with two correction-to-scaling terms. The curvature in the residuals plot is slightly reduced, but the residuals are still not homogeneously distributed. With one correction-to-scaling term, the residuals plot is similar to Figure 5, part a. By adding a third corrective term, the residuals (plot not shown) become more homogeneously distributed.

When β is a free parameter and $T_c = 41.788_5$ °C, large values of β are obtained: $\beta = 0.344 \pm 0.002$ and $\beta = 0.357 \pm 0.002$ with one and two correction-to-scaling terms, respectively.

Fits with β and T_c free are shown in Table 3 (fits 1-b to 3-b). The pure power law gives a critical temperature too low compared to the experimental value. One (Figure 6) and two correction-to-scaling terms give similar χ^2 values and a homogeneous and centered dispersion, within ±2%, of the residuals.

With one correction-to-scaling term, β is close to the 3-D Ising value. With two correction-to-scaling terms, the β value is ~8% larger than the 3-D β-Ising. In either case, the critical temperature given by the fit, within the error estimate ±4 mK, is comparable to that of the experimental T_c value. From these fits, we may conclude that *at least* one correction-to-scaling term can correctly describe the coexistence curve.

Comparison must be made with the fits obtained using the full data set. Fits from the full data set with a pure power law and a power law with one or two correction-to-scaling terms (fit 1-a−3-a, Table 3) always give a large value of the exponent β and a critical temperature larger than the experimental T_c. In Figure 7 we show the residuals for the full data set from the fit 2-b of Table 3 (one correction-to-scaling term, reduced data set) and using the critical temperature given by the fit $T_c = 41.784$ °C. One notices the strong deviation of the residuals for the last four points near T_c. This is the main reason which led us to reject these points.

Remark. We have tested the sensitivity of the value and sign of the amplitude B_1 of the first correction to scaling to the choice of the order parameter. In Table 4 (fits 2 and 3) we show the B_i's amplitudes when the refractive index or the salt mole fraction is used as the order parameter in a two correction-to-scaling terms fit (with T_c and β *fixed*) and using the reduced data set. This analysis shows variations of the value of the second correction-to-scaling amplitude B_2 while the B_1 amplitude remains essentially unchanged. This is in agreement with theoretical studies[35] which show that, for systems which do not strictly obey the O(1) symmetry of the Ising model, additional corrective terms are induced. These terms are controlled by an exponent slightly larger than 2Δ; hence, they are undistinguishable from the second correction-to-scaling term. This may explain the variation of the amplitude B_2 while the amplitude B_1 remains mostly unchanged when the fit is performed using different order parameters.

In Table 4 (fit 4), we also show the result of the one correction-to-scaling fit with the refractive index as the order parameter and when T_c and β are *free*. The sign of the amplitude B_1 is negative and should be compared with the result obtained in the fit 2-b of Table 3 where the volume fraction is the order parameter.

III.B. Effective Exponent. In order to better characterize the effect of the corrections to scaling, it is useful to look at the effective exponent β_{eff} which is defined as follows:

$$\beta_{\text{eff}} = \frac{\partial \ln(\Delta\Phi)}{\partial \ln t} \tag{5}$$

and yields, using eq 3:

$$\beta_{\text{eff}} = \beta_{\text{Ising}} + \frac{\Delta B_1 t^{\Delta} + 2\Delta B_2 t^{2\Delta}}{1 + B_1 t^{\Delta} + B_2 t^{2\Delta}} \tag{6}$$

In general, the ultimate approach of $\beta_{\text{eff}}(t)$ to its asymptotic value (here assumed to be $\beta_{\text{Ising}} = 0.325$), when $t \to 0$, is not universal. In particular, when $B_1 > 0$, the approach is from *above* while it is from *below* when $B_1 < 0$. Experimentally, it has been shown in electrolytic systems that the effective exponent β_{eff} may display a crossover toward the classical value 0.5 as T goes away from T_c.[6,20] This might be explained by the presence of long range interactions in such ionic mixtures. The crossover toward the classical value can be *monotonic*,[20] in which case B_1 is necessarily positive, or *nonmonotonic* with $B_1 < 0$ (see,

TABLE 3: Values of the Parameters Obtained by Fitting the Coexistence Curve with $\Delta\Phi = B_0 t^{\beta}(1 + B_1 t^{\Delta} + B_2 t^{2\Delta})$, See Text[a]

fit	no. of points	T_c (°C)	β	B_0	B_1	B_2	Δ	χ^2
1-a	48	41.790 ± 0.002	0.330 ± 0.002	1.277 ± 0.013				1.06
2-a	48	41.792 ± 0.002	0.348 ± 0.002	1.477 ± 0.015	−0.511 ± 0.10		(0.5)	0.70
3-a	48	41.794 ± 0.002	0.367 ± 0.002	1.737 ± 0.017	−1.572 ± 0.09	3.34 ± 0.6	(0.5)	0.63
1-b	44	41.781 ± 0.004	0.321 ± 0.002	1.234 ± 0.012				1.02
2-b	44	41.784 ± 0.004	0.333 ± 0.002	1.337 ± 0.013	−0.257 ± 0.10		(0.5)	0.93
3-b	44	41.787 ± 0.004	0.352 ± 0.002	1.562 ± 0.015	−1.146 ± 0.09	2.44 ± 0.6	(0.5)	0.90

[a] T_c and β are free parameters in the fitting procedure. Data in parentheses are held fixed in the fitting. Parameter uncertainties are for one standard deviation.

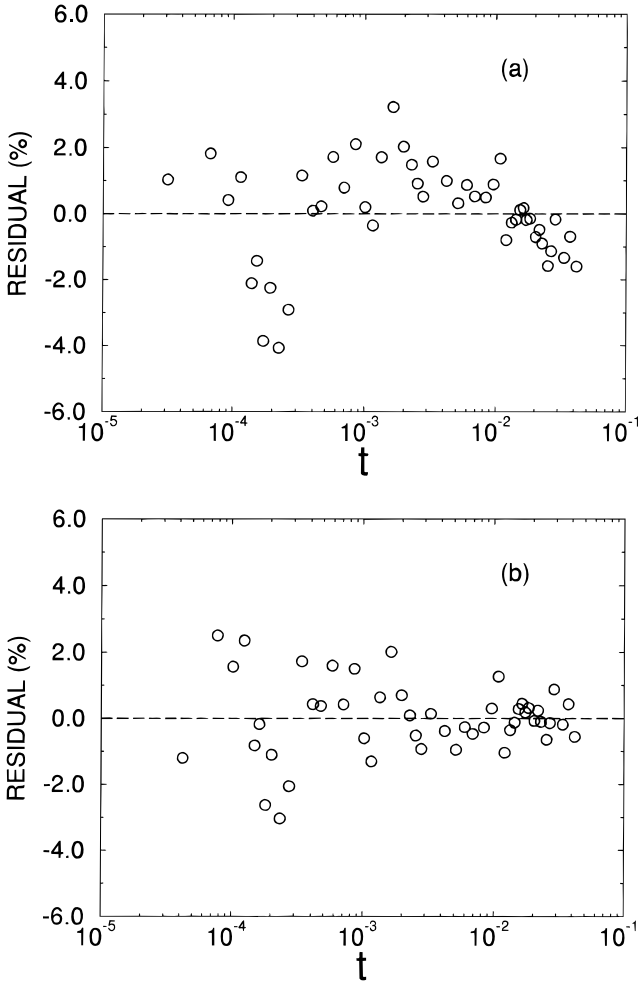

Figure 4. Residuals plot from the fit of the salt volume fraction $\Delta\Phi$ as a function of the reduced temperature t (*full data set*). Fitting with (a) pure power law (fit 1-a, Table 3) and (b) power law and two correction-to-scaling terms (fit 3-a, Table 3). T_c and β are free parameters in the fit.

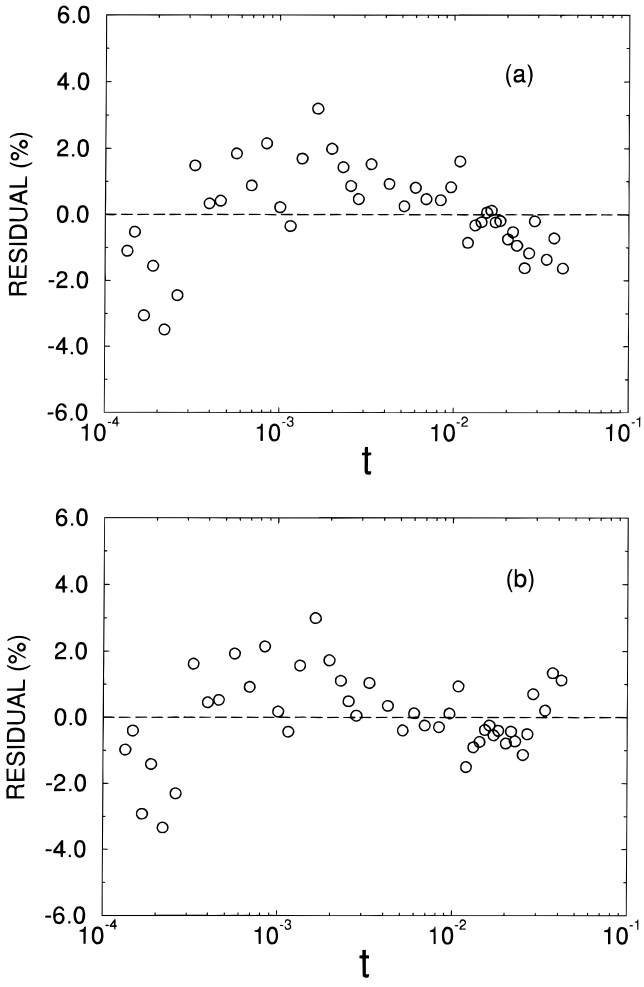

Figure 5. Residuals plot from the fit of the salt volume fraction $\Delta\Phi$ as a function of the reduced temperature t (*reduced data set*). (a) Fitting with a pure power law with $T_c = 41.788_5$ °C and β free parameter (see text). (b) Fitting with two correction-to-scaling terms (fit 3-b, Table 2), with $T_c = 41.788_5$ °C and $\beta = 0.325$ fixed parameters in the fit.

for example, the work of Anisimov *et al.*[36] extended to the case of β_{eff}), in which case the second correction term with positive amplitude B_2 is essential to get the classical β value. The other kinds of approach of β_{eff} to the β-Ising value (such as, for example, with a small $B_1 > 0$ and $B_2 < 0$) are not compatible with a crossover toward a classical value as t grows (more than two correction terms are usually not "observable" in the analysis of actual data).

In the present study, using the full or the reduced data sets does not modify the trend of the effective exponent β_{eff} as a function of temperature. Indeed, the signs of the amplitudes B_1 and B_2 are not modified when fitting with the full or the reduced set (see Tables 2 and 3). Those signs, however, change according to whether T_c and β are let free or not.

In Figure 8, part a, we show β_{eff} (long-dashed curve) computed from the fit 2-b of Table 2 (one correction to scaling, T_c and β fixed in the fitting with the reduced data set). Since B_1 is positive (and small), the approach to the β-Ising value is slightly from above. This could be interpreted as the final approach of a monotonic crossover from a mean-field behavior that would occur at very large values of t. However, B_1 has a small value and is not well defined (a negative value is not excluded), and, moreover, the quality of the fit is not excellent; hence, the approach from above is not well established.

Figure 8, parts a and b (solid curves) show β_{eff} (fit with the reduced data set) when the parameters T_c and β are fixed (with two correction-to-scaling terms, fit 3-b, Table 2) or free (with one correction-to-scaling term, fit 2-b, Table 3), respectively. Figure 8, part a, suggests a possible *nonmonotonic* approach ($B_1 > 0$ and $B_2 < 0$) to the asymptotic 3-D Ising value. The uncertainty estimate of β_{eff} does not allow us to state that this

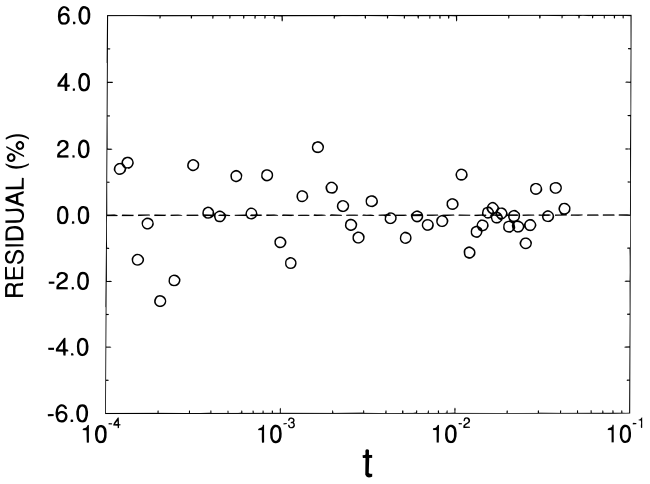

Figure 6. Residuals plot from the fit of the salt volume fraction $\Delta\Phi$ as a function of the reduced temperature t (*reduced data set*). Fitting with a power law and one correction-to-scaling term (fit 2-b, Table 3). T_c and β are free parameters in the fit.

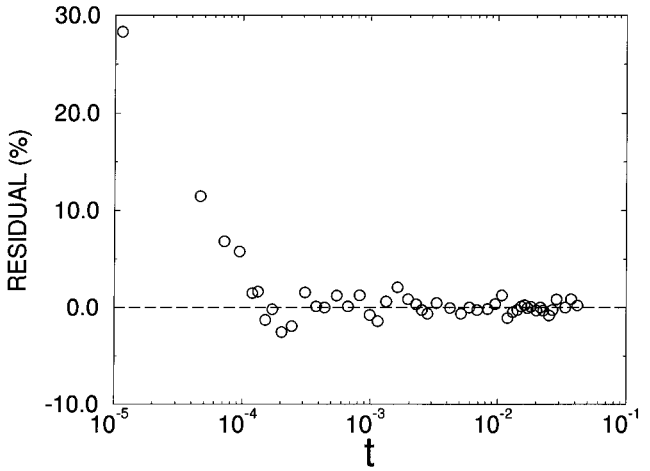

Figure 7. Residuals plot for the *full* data set as a function of the reduced temperature t from a fit computed over the *reduced* data set with one correction-to-scaling term (fit 2-b, Table 3). Notice the strong deviation of four points near T_c not compatible with the homogeneously distributed residuals dispersion ($\approx\pm 2\%$).

kind of approach is an actual characteristic of the system. Complementary measurements (e.g., a light scattering experiment) are at least necessary to check the presence of such a nonmonotonic crossover. At present, we can only remark that both curves (with and without T_c and β fixed) essentially show an approach, from *below*, to the asymptotic value.

Notice that the approach from below for the fit 3-b of Table 2 is not an artifact due to the introduction of the second correction term in a poor converging expansion. Indeed, one may observe that with one term of correction (T_c and β fixed, fit 2-b, Table 2) B_1 is positive but small and a negative value is not excluded, given the uncertainty, and that the introduction of B_2 reduces the χ^2 value. When T_c and β are free, the fits yield a clear monotonic approach from below.

The tendency of the system to find a high value of the asymptotic β value when it is let free (see Table 3) on one hand and the nonmonotonic approach to the Ising value observed when two correction-to-scaling terms are used and the Ising β value is imposed in the fit on the other hand are clearly related.

For completeness, in Figure 8, part a (fit 3-a, Table 2), and Figure 8, part b (fit 2-a, Table 3), we also show the effective exponent β_{eff} which is computed from a fit using the full data set (dotted line): the same kinds of variation of β_{eff} are observed in the same conditions.

We have compared our results with the coexistence curve data obtained from other ionic systems. Figure 9 shows the resulting β_{eff} for the ionic system ($HexEt_3N$ $HexEt_3B$/diphenyl ether)[20] (dotted line, system 1) and for the ionic system (Pe_4-NBr/water)[12] (long-dashed line, system 2) together with our data (solid line, fit 3-b, Table 2). Systems 1 and 2 have been fitted by setting $\beta = 0.325$ and using a two correction-to-scaling terms fit (the parameters of the fit are taken from Table 2, ref 20 and Table 2, ref 12). System 1 shows an evident monotonic crossover from the classical β value of 0.5 to the asymptotic 3-D Ising value with a crossover region located below $t = 10^{-3}$. The decreasing of β_{eff} for $t > 10^{-3}$ may be due to the poor convergence of the power law expansion up to two terms used in the fitting procedure.

Such a monotonic crossover is not observed in system 2 or in the presently studied system. Our system appears more similar to system 2 in that the effective exponent β_{eff} reaches the asymptotic Ising value already for $t \approx 10^{-2}$. The sharp decreasing for the largest values of t is certainly not significant but the trend to go down presumably is.

Uncertainty of the Effective Exponent β_{eff}. From eq 6, near T_c, $\beta_{\text{eff}} \simeq \beta + B_1\Delta t^{\Delta} + B_2 2\Delta t^{2\Delta}$. Here β is the asymptotic β value given by the fit when it is a free parameter or the 3-D Ising value fixed in the fit. The uncertainty of β_{eff} is given by the following:

$$\delta\beta_{\text{eff}} \simeq [(\delta\beta)^2 + (\Delta t^{\Delta}\delta B_1)^2 + (2\Delta t^{2\Delta}\delta B_2)^2 + (\Delta^2 B_1 t^{\Delta-1}\delta t)^2 + (4\Delta^2 B_2 \delta t)^2]^{1/2} \quad (7)$$

where $\delta t = 3 \times 10^{-6}$ is the reduced temperature accuracy and $\delta\beta$, δB_1, and δB_2 are the uncertainties given by Tables 2 and 3. Typical values of $\delta\beta_{\text{eff}}$ are shown in Figure 8, part a and b.

III.C. Diameter of the Coexistence Curve. Considered within the renormalization group theory, the mean diameter $\langle x_i \rangle$, which represents the mean value of the order parameter x_i, should obey the following scaling relation:[29,32]

$$\langle x_i \rangle = \frac{x_{i,\text{l}} + x_{i,\text{u}}}{2} = A_0 + A_1 t + A_2 t^{1-\alpha} + A_3 t^{1-\alpha+\Delta} + \ldots \quad (8)$$

where $x_{i,\text{l}}$ and $x_{i,\text{u}}$ are the values of the order parameter in the lower and upper phases, respectively, and α is the critical exponent of the specific heat c_p. The first two terms on the right-hand side are the regular terms (rectilinear diameter) while the last two terms represent respectively the anomalous and the first correction-to-scaling contributions.

Figure 10, part a, shows the mean diameter $\langle x_n \rangle$ computed from the two-phase refractive indices as a function of temperature (Table 1). A *linear* fit of the mean diameter, far from T_c, has been performed within the temperature range 3.01 °C < ($T_c - T$) < 13.13 °C ($9.6 \times 10^{-3} \le t \le 4.2 \times 10^{-2}$). Extrapolation of the rectilinear diameter to $T_c = 41.788_5$ °C (intercept, Figure 10, part a) gives the value of the refractive index at T_c, $n_c = 1.435\,51 \pm 0.000\,03$.

A linear extrapolation to T_c of the refractive index measured in the one-phase region within 7 mK < ($T - T_c$) < 6.798 K (Table 1) gives $n_c = 1.435\,72 \pm 0.000\,02$. The difference between these two values ($\Delta n_c \approx 0.0002$) is comparable to the absolute accuracy of the refractive index measurement. This indicates clearly that the mixture is at the critical concentration.

In Figure 10, part b, we show the same analysis performed on the mean diameter $\langle x_s \rangle$ computed from the salt mole fraction. Comparison of the extrapolated rectilinear diameter to T_c with the known experimental critical mole fraction can thus be done.

TABLE 4: Value of the B_i Amplitudes Obtained from a Two Correction-to-Scaling Terms Fit (*Reduced* Data Set) When Different Order Parameters Are Used To Describe the Coexistence Curve[a]

fit	order parameter	T_c (°C)	β	B_0	B_1	B_2
1	salt volume fraction	(41.788_5)	(0.325)	1.219 ± 0.019	0.65 ± 0.16	-3.0 ± 1.0
2	salt molar fraction	(41.788_5)	(0.325)	0.812 ± 0.020	0.78 ± 0.27	-1.5 ± 1.8
3	refractive index	(41.788_5)	(0.325)	0.0155 ± 0.0004	0.64 ± 0.25	-5.0 ± 1.6
4	refractive index	41.786 ± 0.006	0.346 ± 0.003	0.0189 ± 0.0003	-0.90 ± 0.13	

[a] Data in parentheses are held fixed in the fitting. Fits 2 and 3 should be compared to fit 1 (same as fit 3-b of Table 2). In both cases one may observe a rather good stability of B_1. Fit 4 should be compared to fit 2-b of Table 3.

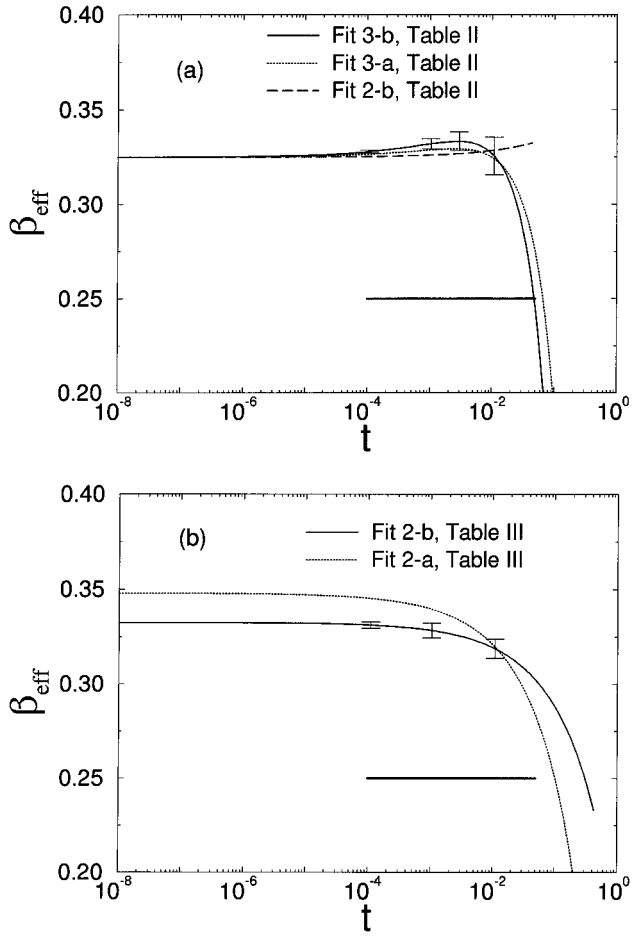

Figure 8. Effective exponent β_{eff}, eq 6, as a function of the reduced temperature t. (a) Fit with *two* correction-to-scaling terms. Solid line: *reduced* data set (fit 3-b, Table 2). Dotted line: *full* data set (fit 3-a, Table 2). Fit with *one* correction-to-scaling term: long-dashed line, *reduced* data set (fit 2-b, Table 2). $T_c = 41.788_5$ °C and $\beta = 0.325$ are fixed parameters. (b) Fit with *one* correction-to-scaling term and T_c and β free parameters in the fit. Solid line: *reduced* data set (fit 2-b,Table 3). Dotted line: *full* data set (fit 2-a, Table 3). The horizontal bar indicates the experimental temperature region where the fit has been performed.

The extrapolation to T_c (intercept, Figure 10, part b) gives a salt mole fraction $x_s = 0.769 \pm 0.001$ which compares favorably well, within 0.4%, with the experimental value used to fill the cell $x_{s,c} = 0.766 \pm 0.002$.

A linear extrapolation to T_c of the salt mole fraction computed in the one-phase region gives $x_s = 0.780 \pm 0.0005$. However, this value is higher by 1.8% from the salt mole fraction $x_{s,c}$. This 1.8% difference is comparable to the estimated mole fraction accuracy (∼1% near T_c).

Figure 10, part b, clearly shows a systematic deviation from the rectilinear law of the salt mole fraction mean diameter when $(T_c - T) < 3$°C, which is analyzed in more details below. Instead of fitting the mean diameter with eq 8 and, due to the difficulty of accurately separating the regular contribution from the critical one because of the comparable values of the

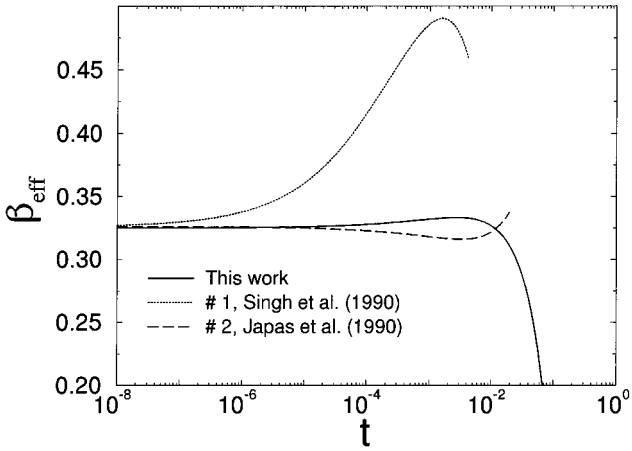

Figure 9. Effective exponent β_{eff}, eq 6, as a function of the reduced temperature t. Solid curve, this work (fit 3-b, Table 2); dotted curve, ionic system ($HexEt_3N$ $HexEt_3B$/diphenyl ether)[20]; long-dashed curve, water solution of Pe_4NBr.[12]

exponents, we first subtract from the mean diameter the linear contribution. Figure 11 shows the deviation from the rectilinear law:

$$\Delta x = \langle x_s \rangle - (a_0 + a_1(T_c - T)) \qquad (9)$$

with $a_0 = 0.769$ and $a_1 = -0.00567$ K^{-1} obtained from the linear regression.

Two different behaviors of Δx can be noticed when $(T_c - T) < 3$ °C. With 0.2 °C $< (T_c - T) < 3$ °C, we observe an exponential increase of Δx (see Figure 11), followed by a leveling-off and a slight decrease of Δx for $(T_c - T) <$ 0.1 °C. This exponential increase has been observed by Gopal *et al.*[28] in nonionic binary mixtures and is not attributable to gravity effects. As suggested by these authors, the deviation from the rectilinear law may be fitted by the following equation:

$$\Delta x = b_0(T_c - T)^{b_1} \exp(-b_2(T_c - T)^{b_3}) \qquad (10)$$

where the b_i's are the parameters to be determined. When $(T_c - T) \rightarrow 0$, the critical term $b_0(T_c - T)^{b_1}$ is the dominant term in eq 10. We let b_1 a free parameter ($b_1 \approx 0.09$, dotted curve, Figure 11) or fixed to $(1 - \alpha) = 0.89$ (long-dashed curve, Figure 11). With $b_1 = (1 - \alpha) = 0.89$, the fit gives $b_0 = 2.23$, $b_2 = 6.31$, and $b_3 = 0.26$. From Figure 11, it appears that the critical anomaly of the diameter might be observable only in a very narrow region near T_c, i.e., for $(T_c - T) < 0.1$ °C ($t \leq 3 \times 10^{-4}$).

This analysis shows that far away from T_c the mean diameter is rectilinear with a $(1 - \alpha)$-type critical anomaly near T_c. Due to the lack of precision of our measurements in this domain and to the small amplitude of the critical anomaly term ($\Delta x \approx$ 1%), we cannot determine accurately the critical exponent. In the intermediate region, the deviation from the rectilinear diameter can be fitted by an exponential law.

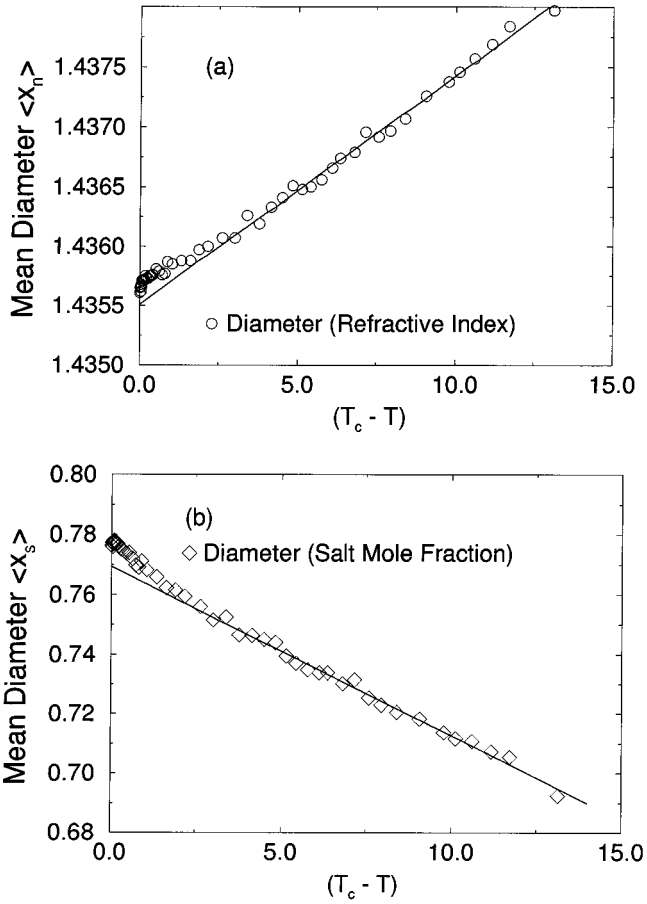

Figure 10. Mean diameter as a function of the reduced temperature t. (a) $\langle x_n \rangle$ computed from the refractive index and (b) $\langle x_s \rangle$ computed from the salt mole fraction. The mean diameter is fitted with a linear law in the temperature range 3.1 °C < T_c − T < 13.13 °C (solid line). T_c = 41.788$_5$ °C.

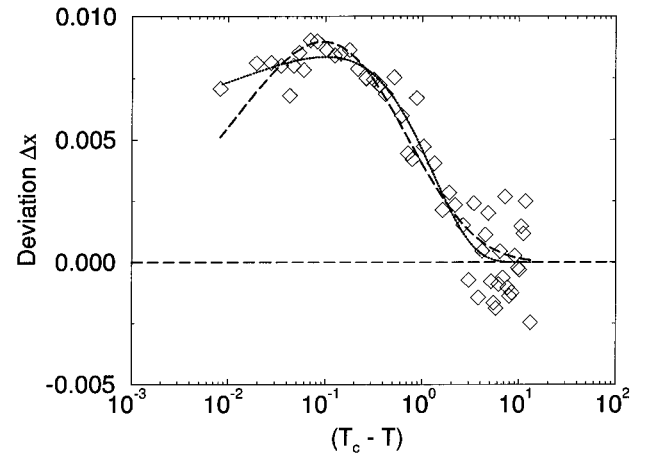

Figure 11. Deviation Δx from the rectilinear diameter (eq 9) as a function of temperature (T_c = 41.788$_5$ °C). Diamonds: experimental points (salt mole fraction). Dotted curve: fitting with eq 10 and exponent b_1 as a free parameter. Long-dashed curve: fitting with eq 10 and $b_1 = (1 - \alpha) = 0.89$ as a fixed parameter. Notice that the diameter anomaly term is important for ($T_c - T$) < 0.3 °C (around the maxima of the curves).

IV. Conclusion

Measurements of the coexistence curve of the ionic system ethylammonium nitrate−*n*-octanol have been made in a reduced temperature range $2.6 \times 10^{-5} < t < 4.2 \times 10^{-2}$. The salt volume fraction, which gives the more symmetric coexistence curve, is the appropriate order parameter to correctly analyze the coexistence curve. Fitting of the coexistence curve was performed within two temperature ranges: $2.6 \times 10^{-5} < t < 4.2 \times 10^{-2}$ and $10^{-4} < t < 4.2 \times 10^{-2}$.

The asymptotic β value is found to be close to the 3-D Ising value. In order to determine a possible crossover from the classical value $\beta = 0.5$ to the Ising value as t decreases, the effective exponent β_{eff} has been computed as a function of the reduced temperature. It appears that no trend toward a classical value is observed since the asymptotic Ising value is rather approached *from below*. The present ionic system has a larger asymptotic domain compared to the ionic system ($HexEt_3N$ $HexEt_3B$/diphenyl ether).[20] The observed weak *nonmonotonic* behavior requires validation by other studies on this system. With respect to the water solution of tetra-*n*-pentylammonium bromide,[12] the asymptotic region has a similar extension. The presence of hydrogen bonds between anions in the EAN-*n*-octanol mixture,[37] overshadowing the Coulombic interaction, might explain the relatively large asymptotic region although a relationship between the range of interaction, such as an ion−dipole interaction in a water electrolytic solution, and the range of crossover is not straightforward as is evidenced by the experiment of Japas *et al.*[12]

Our result also confirms the conclusion of Weingärtner *et al.*[17] who have observed, by light scattering, that no crossover to a classical value could be evidenced.

A deviation from the rectilinear diameter is observed for $t < 10^{-2}$. The effect of a possible $(1 - \alpha)$ anomaly can be observed within a very narrow range of temperature for $t < 3 \times 10^{-4}$. Due to the lack of accuracy of the measurements near T_c, we are not able to determine precisely the exponent of the critical diameter anomaly.

Acknowledgment. We thank Y. Garrabos for fruitful discussions and a careful reading of the manuscript and P. Guénoun for useful comments.

References and Notes

(1) Pitzer, K. S. *Acc. Chem. Res.* **1980**, *13*, 333.
(2) Levelt Sengers, J. M. H.; Given, J. A. *Mol. Phys.* **1993**, *80*, 889.
(3) Weingärtner, H.; Kleemeier, M.; Wiegand, S.; Schröer, W. *J. Stat. Phys.* **1995**, *78*, 169.
(4) Fisher, M. E. *J. Stat. Phys.* **1994**, *75*, 1.
(5) Bockris, J. O'M.; Reddy, A. K. N. *Modern Electrochemistry*; Plenum: New York, 1970.
(6) Narayanan, T.; Pitzer, K. S. *J. Chem. Phys.* **1995**, *102*, 8118.
(7) Weingärtner, H.; Merkel, T.; Maurer, U.; Conzen, J.-P.; Glasbrenner, H.; Käshammer, S. *Ber. Bunsen-Ges. Phys. Chem.* **1991**, *95*, 1579.
(8) Xu, H.; Friedman, H. L.; Raineri, F. O. *J. Solution Chem.* **1991**, *20*, 739.
(9) Kunz, W.; Calmettes, P.; Turq, P. *J. Chem. Phys.* **1990**, *92*, 2367.
(10) Kunz, W.; Turq, P.; Calmettes, P.; Barthel, J.; Klein, L. *J. Phys. Chem.* **1992**, *96*, 2743.
(11) Kunz, W.; Calmettes, P.; Cartailler, T.; Turq, P. *J. Chem. Phys.* **1993**, *99*, 2074.
(12) Japas, M. L.; Levelt Sengers, J. M. H. *J. Phys. Chem.* **1990**, *94*, 5361.
(13) Evans, D. F.; Yamauchi, A.; Roman, R.; Casassa, E. Z. *J. Colloid Interface Sci.* **1982,** *88*, 89.
(14) Perron, G.; Hardy, A.; Justice, J.- C.; Desnoyers, J. E. *J. Solution Chem.* **1993**, *22*, 1159.
(15) Schröer, W.; Wiegand, S.; Weingärtner, H. *Ber. Bunsen-Ges. Phys. Chem.* **1993**, *97*, 975.
(16) Bonetti, M.; Bagnuls, C.; Bervillier, C. Submitted for publication to *J. Chem. Phys.*
(17) Weingärtner, H.; Merkel, T.; Kashammer, S.; Schröer, W.; Wiegand, S. *Ber Bunsen-Ges. Phys. Chem.* **1993**, *97*, 970.
(18) Pitzer, K. S.; Conceicao, M.; de Lima, P.; Schreiber, D. R. *J. Phys. Chem.* **1985**, *89*, 1854.
(19) Singh, R. R.; Pitzer, K. S. *J. Am. Chem. Soc.* **1988**, *110*, 8723.
(20) Singh, R. R.; Pitzer, K. S. *J. Chem. Phys.* **1990**, *92*, 6775.
(21) Oleinikova, A.; Bonetti, M. *J. Chem. Phys.* **1996**, *104*, 3111.
(22) Letellier, P. (private communication).
(23) Jacobs, D. T.; Anthony, D. J.; Mockler, R. C.; O'Sullivan, W. J. *Chem. Physics* **1977**, *20*, 219.
(24) Houessou, C.; Guénoun, P.; Gastaud, R.; Perrot, F.; Beysens, D. *Phys. Rev. A* **1985**, *32*, 1818.

(25) Moldover, M. R. *Phys. Rev. A* **1985**, *31*, 1022.
(26) Chan, C. K.; Goldburg, W. I. *Phys. Rev. Lett.* **1987**, *58*, 674. Beysens, D. *Comments Condens. Mater. Phys.* **1991**, *15*, 201.
(27) To, C. W.; Chan, C. K. *Europhys. Lett.* **1993**, *24*, 365.
(28) Gopal, E. S. R.; Chandra Sekhar, P.; Ananthakrishna, G.; Ramachandra, R.; Subramanyam, S. V. *Proc. R. Soc. London A* **1976**, *350*, 91.
(29) Kumar, A.; Krishnamurthy, H. R.; Gopal, E. S. R. *Phys. Rep.* **1983**, *98*, 57.
(30) Andrew, W. V.; Khoo, T. B. K.; Jacobs, D. T. *J. Chem. Phys.* **1986**, *85*, 3985.
(31) Wegner, F. J. *Phys. Rev. B* **1972**, *5*, 4529.
(32) Ley-Koo, M.; Green, M. S. *Phys. Rev. A* **1981**, *23*, 2650.
(33) Minuit Cern (V94.1, Geneva) fitting routines (Monte Carlo minimization using Metropolis algorithm) have been used for data reduction.
(34) Zinn-Justin, J. *Euclidean Field Theory and Critical Phenomena*; Clarendon Press: Oxford, 1989.
(35) Mermin, N. D.; Rehr, J. J. *Phys. Rev. Lett.* **1971**, *26*, 1155. Nicoll, J. F. *Phys. Rev. A* **1981**, *24*, 2203. Zhang, F. C.; Zia, R. K. P. *J. Phys. A* **1982**, *15*, 3303. Anisimov, M. A.; Gorodetskii, E. E.; Kulikov, V. D.; Sengers, J. V. *Phys. Rev. E* **1995**, *51*, 1199.
(36) Anisimov, M. A.; Povodyrev A. A.; Kulikov, V. D.; Sengers, J. V. *Phys. Rev. Lett.* **1995**, *75*, 3146.
(37) Evans, D. F.; Chen, S.-H.; Schriver, G. W.; Arnett, E. M. *J. Am. Chem. Soc.* **1981**, *103*, 481.